

COMMUNICATION

[View Article Online](#)
[View Journal](#) | [View Issue](#)

 Cite this: *Phys. Chem. Chem. Phys.*,
 2016, 18, 17351

 Received 22nd April 2016,
 Accepted 8th June 2016

DOI: 10.1039/c6cp02706g

www.rsc.org/pccp

It is explicitly verified that the atomic $7p^1$ ground-state configuration of Lr originates from relativistic effects. Without relativity one has $6d^1$. All three ionization potentials IP_{1-3} of Lr resemble those of Lu. Simple model studies on mono- and trihydrides, monocarbonyls or trichlorides suggest no major chemical differences between Lr and the lanthanides.

1 Introduction

The periodic table is about chemistry. The group is related to the number of valence electrons and the period is related to the number of nodes in the radial functions of these electrons. In lawrencium, ^{103}Lr , counting the filled 5f shell as the 'core', there are three valence electrons. It had been debated for some time, whether they are $7s^26d^1$ or $7s^27p_{1/2}^1$, until both an experiment¹ and also the latest calculations supported the latter alternative. That $7p^1$ atomic ground state was first surmised by Brewer² and first calculated by Desclaux and Fricke.³ Large MCDF calculations by Zou and Froese Fischer⁴ support the $5d^1$ and $7p^1$ ground states for Lu and Lr, respectively, and yield very different oscillator strengths. For Lr, however, they are not yet experimentally confirmed.

This does not yet settle the question on the chemical behaviour. If all three valence electrons are formally ionized away, in an Lr(III) compound, lawrencium clearly belongs to Group 3 in Period 7, and nothing unexpected has happened in its chemistry.

The three first ionization potentials of Lr are compared with those of La–Lu in Fig. 1. They are quite similar, especially with Lu. Therefore the ionic chemistry of Lr could be expected to be similar to that of the lanthanides.

Lr versus Ln atomic IP

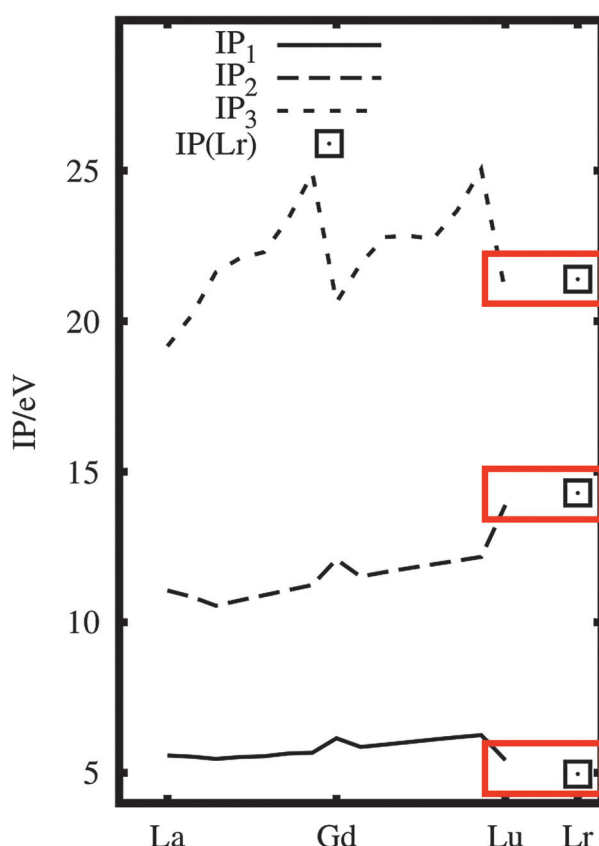


Fig. 1 The ionization potentials of La–Lu (experimental data⁵) and Lr (experimental and calculated $IP_{1,1}$, calculated $IP_{2,3}$ ⁶). Note the similarity of Lu and Lr.

^a Key Laboratory of Synthetic and Natural Functional Molecule Chemistry of the Ministry of Education, College of Chemistry and Molecular Science, Northwest University, 710127 Xi'an, China. E-mail: xuwenhua.qf@gmail.com

^b Department of Chemistry, University of Helsinki, POB 55 (A. I. Virtasen aukio 1), 00014 Helsinki, Finland. E-mail: Pekka.Pyykko@helsinki.fi

† Electronic supplementary information (ESI) available. See DOI: 10.1039/c6cp02706g

Experimentally this is what happened, see Brüchle *et al.*,⁷ Hoffman *et al.*,⁸ and Scherer *et al.*,⁹ all in 1988. Brüchle and Hoffman found that Lr(III) had a similar elution behaviour to the latter Ln(III) and Scherer found no evidence for a possible reduction to lower oxidation states than Lr(III) in aqueous

solution. Recently, in reductive surroundings, all the divalent lanthanide oxidation states $\text{Ln}(\text{II})$ have also been obtained.¹⁰ These divalent lanthanide, $\text{Ln}(\text{II})$, compounds are mostly 5d^1 . No such experiments exist on Lr.

Calculations suggest that the free-atom $\text{Lr}(\text{i})$ and $\text{Lr}(\text{II})$ are 7s^2 and 7s^1 , respectively,^{5,6,11} in contrast to the quoted 5d^1 for $\text{Ln}(\text{II})$ in compounds.¹⁰ The stabilisation of the 7s shell in Group 3 can be compared with that of the 6s shell in Group 13, which contributes to the chemical difference between indium and thallium, having the main oxidation states $\text{In}(\text{III})$ and $\text{Ti}(\text{i})$, respectively. Similarly, for lead, the relativistic stabilization of the 6s shell favours the divalent $\text{Pb}(\text{II})$ state in PbO or PbSO_4 and destabilizes the $\text{Pb}(\text{IV})$ state in PbO_2 , thereby explaining most of the voltage of the lead battery.¹² In these main-group cases the relativistic stabilization of an ns shell leads to different main oxidation states in Periods 5 and 6. One possibility considered here is whether one could have a similar change between lanthanides and actinides. Recall that the relativistic stabilization of valence s shells down the same column increases as Z^2 , where Z is the nuclear charge.

2 Atomic results

We first verify the relativistic origin of the ground-state change from 6d^1 to 7p^1 , see Table S1 in the ESI.† Compared with the non-relativistic results, Dirac–Fock (DF) shifts down the relative energy of $(n+1)^2\text{P}$ to $n^2\text{D}$ by nearly 3 eV, and changes the ground state configuration. The relativistic effect is so large that already DF-level evidence makes sense. MCDF results were reported by Fritzsche *et al.*¹³

The calculated orbital energies for Tl and Lr atoms are shown in Fig. 2. It is seen that the relativistic stabilization of the Tl 6s shell is substantial, making its energy comparable to the ligand orbital energy (here H). In contrast, the Lr 7s orbital energy is small, despite a larger Z .

Does the atomic ground state matter in chemistry? As seen in Fig. 2, the valence orbital energies of the electropositive element Lr are small and hence in compounds these electrons, whether 7s , 6d or 7p , will largely go away, anyway. Group 13 is more electronegative¹⁴ than Group 3.

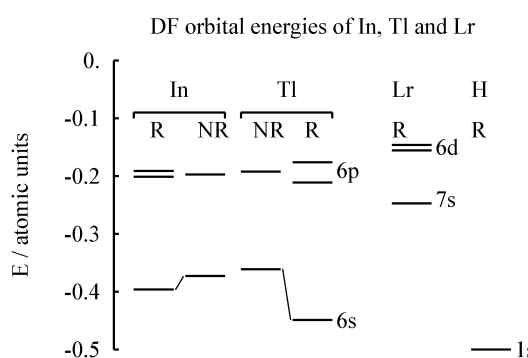


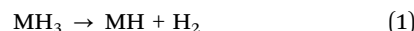
Fig. 2 The calculated relativistic (R) and non-relativistic (NR) Dirac–Fock orbital energies of neutral In, Tl and Lr atoms. For lawrencium, the electron configuration $7\text{s}^26\text{d}^1$ is assumed. Values from Desclaux.¹⁵

Why is Lr, like other lanthanides and actinides, so electropositive? A broad-brush explanation could be that they all belong to Group 3 and the electronegativities in the Periodic table increase from left to right (from Group 1 to Group 18), probably due to increasing partial screening by the fellow valence electrons.

3 Molecular results

3.1 Hydrides

We first consider the simple hydride models and calculate the reaction energy, ΔE for the model reaction



for $\text{M} = \text{Lr, Lu, In}$ and Tl . As seen in Table 1, this ΔE is negative for thallium which clearly prefers to be $\text{Tl}(\text{i})$, and positive for the other four metals, which prefer being $\text{M}(\text{III})$, including $\text{Lr}(\text{III})$. $\text{Tl}(\text{i})$ is an example of the relativistic 6s^2 inert pair.

The structural parameters are given in Table 2.

3.2 Monocarbonyls

We then compare LrCO with the series LnCO , $\text{Ln} = \text{La–Lu}$, studied both experimentally and theoretically by Xu *et al.*¹⁹ There the three last members $\text{Ln} = \text{Tm, Yb, and Lu}$ which could not be made, and they had theoretically weak bonds, for Lu with a $\sigma^2\pi^1$ valence configuration. We now find that Lr behaves just like Lu, which further supports putting it under Lu in the

Table 1 Reaction energies ΔE for $\text{MH}_3 \rightarrow \text{MH} + \text{H}_2$ (1) (in eV). The In and Tl results are from Vest *et al.*¹⁶ The other results from the present work. As seen from Table 2, LrH_3 is C_{3v}

M	HF	MP2	CCSD(T)	DFT
Lr	+0.17	-0.07	+0.10	+0.39
Lr^a	+0.14	-0.03	+0.13	
Ac	+0.44	+0.10	+0.25	+0.89
Lu	+0.88	+0.66	+0.72	+0.91
In			+0.07	
Tl			-0.72	

^a Triple-zeta basis. Other wave function methods use the double-zeta basis.

Table 2 Geometrical two-component (2c) DFT parameters of MH , MH_2 , MH_3 , MCO , MCl_3 and $[(\text{Cp}')_3\text{M}]^-$ ($\text{M} = \text{Lu, Lr}$). Lengths in Å, angles in degrees

Molecule	Symmetry	Bond length	Bond angle
LuH	Linear	1.895	
LrH	Linear	1.960	
LuH_2	C_{2v}	1.915	113.5
LrH_2	C_{2v}	1.954	110.6
	C_{2v}^a	2.015	117.5
LuH_3	C_{3v}	1.921	112
LrH_3	C_{3v}	1.940	107
LuCO	Linear	2.297 (Lu–C), 1.167	180
LrCO	Linear	2.384 (Lr–C), 1.169	180
LuCl_3	D_{3h}	2.394	120
LrCl_3	C_{3v}	2.424	113
$[(\text{Cp}')_3\text{Lu}]^-$	C_1	2.635 ^{b,c}	
$[(\text{Cp}')_3\text{Lr}]^-$	C_1	2.697 ^c	

^a Ref. 17. ^b Ref. 10. ^c Shortest M–C.



Table 3 Population analysis of LrH , LrH_2 , LrH_3 , LuCO and LrCO . P: projection analysis;¹⁸ M: Mulliken population. G: Four-component Hamiltonian with the DZ Gaussian basis set; S: two-component Hamiltonian with the DZ Slater basis set

Mol.	Type	Functional	Valence population
LuH	P, G	PBE	$\text{Lu 6s}(1.78)5\text{d}(0.71)6\text{p}(0.22) \text{H 1s}(1.26)$
	M, S	PBE	$\text{Lu 6s}(1.77)5\text{d}(0.68)6\text{p}(0.20) \text{H 1s}(1.34)$
LrH	P, G	PBE	$\text{Lr 7s}(1.82)6\text{d}(0.63)7\text{p}(0.28) \text{H 1s}(1.25)$
	P, G	PBE0	$\text{Lr 7s}(1.80)6\text{d}(0.57)7\text{p}(0.28) \text{H 1s}(1.30)$
LuH_2	P, G	CAMB3LYP	$\text{Lr 7s}(1.80)6\text{d}(0.53)7\text{p}(0.27) \text{H 1s}(1.34)$
	M, S	PBE	$\text{Lr 7s}(1.83)6\text{d}(0.61)7\text{p}(0.21) \text{H 1s}(1.34)$
LrH_2	M, S	PBE	$\text{Lu 6s}(1.03)5\text{d}(0.96)6\text{p}(0.27) \text{H 1s}(1.35)$
	M, S	PBE	$\text{Lr 7s}(1.19)6\text{d}(0.87)7\text{p}(0.25) \text{H 1s}(1.33)$
LuH_3	P, G	PBE	$\text{Lu 6s}(0.74)5\text{d}(1.06)6\text{p}(0.27) \text{H 1s}(1.29)$
	M, S	PBE	$\text{Lu 6s}(0.66)5\text{d}(0.97)6\text{p}(0.25) \text{H 1s}(1.36)$
LrH_3	P, G	PBE	$\text{Lr 7s}(0.89)6\text{d}(1.05)7\text{p}(0.25) \text{H 1s}(1.26)$
	M, S	PBE	$\text{Lr 7s}(0.84)6\text{d}(0.94)7\text{p}(0.17) \text{H 1s}(1.34)$
LuCO	M, S	PBE	$\text{Lu 6s}(1.77)5\text{d}(0.75)6\text{p}(0.18) \text{C 2sp}(3.90) \text{O 2sp}(6.25)$
LrCO	M, S	PBE	$\text{Lr 7s}(1.82)6\text{d}(0.66)7\text{p}(0.20) \text{C 2sp}(3.91) \text{O 2sp}(6.27)$

Table 4 Natural electron configurations of LrH , LrH_3 , LuCO and LrCO . The density matrices are from ZORA1c and PBE calculations. At this level, an NBO was available

Mol.	Natural electron configuration
LrH	$[\text{core}]7\text{s}(1.92) 6\text{d}(0.34) 7\text{p}(0.04)$
LrH_3	$[\text{core}]7\text{s}(0.84) 6\text{d}(0.67) 7\text{p}(0.01)$
LrCO	$[\text{core}]7\text{s}(1.93) 6\text{d}(0.51) 7\text{p}(0.05)$
LuCO	$[\text{core}]6\text{s}(1.90) 5\text{d}(0.56) 6\text{p}(0.06)$

Periodic table. At the CCSD(T) level, LrCO is 1.0 eV below $\text{Lr} + \text{CO}$, while LuCO is 0.77 eV below $\text{Lu} + \text{CO}$. The attempts to produce LuCO ¹⁹ nevertheless failed.

Population analyses are shown in Tables 3–5. Projection analysis is stable regarding different types of functionals. In this study, Mulliken populations agree well with the projection analysis. There is a high correlation between Lu and Lr electronic configurations in all the hydrides and carbonyls.

The C–O stretching frequencies are 1897 and 1921 cm^{-1} for LrCO and LuCO , respectively. The valence orbitals of LuCO and LrCO are compared in Fig. 3 and found to be very similar. We conclude that although the p populations strongly depend on the method of calculation, Mulliken, NBO (Natural Bond Orbital) or projection, the results for Lu 6p and Lr 7p are closely similar.

Table 5 Frontier HF orbitals of LrH , LrH_3 , LuCO and LrCO . The first two closed-shell molecules are computed using an X2C Hamiltonian, while the latter two open-shell ones use a scalar relativistic ECP. Energies in eV. Mulliken populations in %. h = HOMO. At the spin–orbit-split two-component level, only Mulliken population analysis was available

Mol.	Orb.	Energy	Populations
LrH	h	−6.31	$\text{Lr s}(64), \text{Lr p}(14), \text{Lr d}(13), \text{H s}(7)$
	h-1	−10.61	$\text{Lr s}(28), \text{Lr p}(5), \text{Lr d}(10), \text{H s}(56)$
LrH_3	h	−9.65	$\text{Lr p}(8), \text{Lr d}(26), \text{H s}(67)$
	h-1	−10.16	$\text{Lr p}(14), \text{Lr d}(18), \text{H s}(65)$
LrCO	h	−11.65	$\text{Lr s}(39), \text{H s}(55)$
	h-1	−6.31	$\text{Lr p}(10), \text{Lr d}(26), \text{C p}(47), \text{O p}(16)$
LuCO	h	−6.92	$\text{Lr s}(86), \text{Lr p}(7), \text{Lr d}(6)$
	h-1	−6.72	$\text{Lu p}(11), \text{Lu d}(23), \text{C p}(44), \text{O p}(15)$
		−6.38	$\text{Lu s}(84), \text{Lu p}(8), \text{Lu d}(8)$

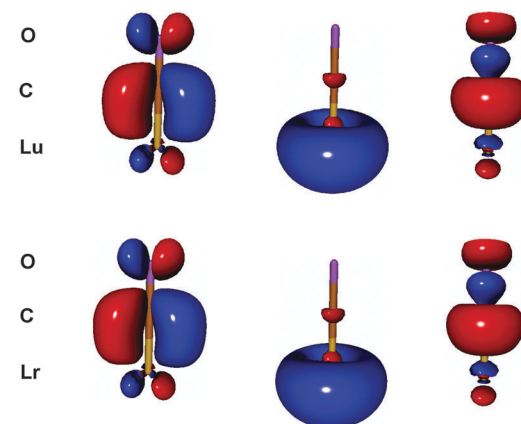


Fig. 3 The HF π (HOMO), σ (HOMO−1) and σ donation molecular orbitals (from left to right) of the monocarbonyls LuCO and LrCO with ECP. They are fairly similar to each other.¹⁹ Isodensity value = 0.05 a.u.

3.3 Lawrencium trichloride and a divalent complex

One feature of the bonding in lanthanide chlorides is the π – d bond. It is also observed in LrCl_3 . Note that unlike in D_{3h} LuCl_3 , the geometry of LrCl_3 is C_{3v} , with an out-of-plane vibrational frequency of only 48 cm^{-1} . For the bonding molecular orbitals, see Fig. 4.

In recent years, one breakthrough in lanthanide chemistry is that divalent complexes were synthesized and characterized for all lanthanides. We now studied an Lr complex with the same ligand as that for Ln, i.e. $\text{C}_5\text{H}_4\text{SiMe}_3$ (Cp'). Experimentally, a potassium atom in a crown ether¹⁰ functioned as the counterion of $[\text{Ln}(\text{Cp}')_3]^-$.

A stable geometry was found for this complex anion. The electronic structure is similar to that of Lu. The metal configuration is 6d^1 . Spin–orbit effects were included in the calculation. As seen from Fig. 5, this HOMO is a d^1 orbital on Lr.

The structures of all systems are given in the ESI.†

4 Relation to the periodic table

Three different choices can be outlined for the f-element rows:

- Fourteen-element rows, La–Yb and Ac–No. Put Lu and Lr in Group 3. Chosen by Jensen²⁰ and currently Wikipedia.



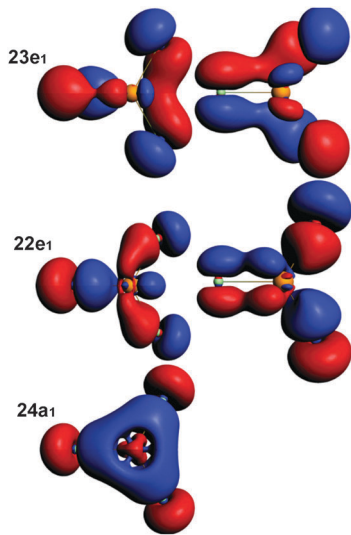


Fig. 4 The molecular orbitals of the C_{3v} LrCl_3 with $3p(\text{Cl})$ – $6d(\text{Lr})$ bonds. They are fairly similar to those of LuCl_3 . The 'e' orbitals are doubly degenerate and both components are shown. Isodensity value = 0.05.

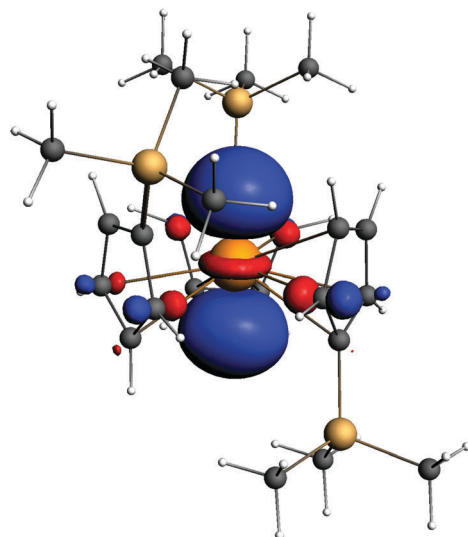


Fig. 5 The HOMO orbital of $[(\text{Cp}')_3\text{Lr}]^-$. Isodensity value = 0.05 a.u.

2. Fourteen-element rows, Ce–Lu and Th–Lr. Put La and Ac in Group 3. Chosen by Lavelle,²¹ the Royal Society of Chemistry and the American Chemical Society.

3. Fifteen-element rows, La–Lu and Ac–Lr. This includes f^0 among the f^1 to f^{14} series. All elements are mostly trivalent. Their ionic and covalent²² radii form a continuous series. Now chosen by IUPAC²³ and by us. To us the atomic ground state is less important than the chemical bonding, in the systems so far considered.

5 Computational details

The geometries were optimized at the ZORA2c²⁴ level, DFT (PBE functional²⁵) with TZ2P²⁶ Slater basis sets. The vibrational

frequencies were obtained to confirm the minima. However, $[(\text{Cp}')_3\text{Lr}]^-$ was optimized with the TPSSh functional^{27,28} to compare with the published $[(\text{Cp}')_3\text{Lu}]^-$ results. Solvent effects were considered by the COSMO model²⁹ with tetrahydrofuran (THF) parameters. For more details, see the computational part of ref. 10. ADF 2016^{30,31} and Turbomole 7.02³² packages were used. To calculate more accurate energetics, the two-component (2c)-MP2^{33,34} and (2c)-CCSD(T)³⁵ as implemented in Dirac 15.0,³⁶ and CCSD(T) implemented in Molpro 2015.1^{37,38} were employed. The basis sets are Dyall all-electron double zeta³⁹ and ECP from the Stuttgart/Cologne group,^{40,41} respectively.

6 Conclusion

All three ionization potentials of the lawrencium atom resemble those of the lanthanides, especially lutetium. Despite the different atomic ground states of d^1 and $(p^*)^1$ for Lu and Lr, respectively, their chemical behaviour in the present systems is found to be similar. Nothing prevents one from keeping a fifteen-element trivalent actinide row Ac–Lr, under the trivalent lanthanide row La–Lu. This entirely avoids the issues arising from fourteen-element rows.^{20,21}

Acknowledgements

This project is supported by grant 275845 from The Academy of Finland to Professor Dage Sundholm. WHX thanks the China Scholarship Council and the Northwest University, Xi'an for a leave of absence and support (No. 13NW24). CSC, Espoo, Finland, provided both software and computer time. PP is grateful to the Magnus Ehrnrooth Foundation for a travel grant.

References

- 1 T. K. Sato, M. Asai, A. Borschevsky, T. Stora, N. Sato, Y. Kaneya, K. Tsukada, Ch. E. Düllmann, K. Eberhardt, E. Eliav, S. Ichikawa, U. Kaldor, J. V. Kratz, S. Miyashita, Y. Nagame, K. Ooe, A. Osa, D. Renisch, J. Runke, M. Schädel, O. Thörle-Pospiech, A. Toyoshima and N. Trautmann, *Nature*, 2015, **520**, 209–211.
- 2 L. Brewer, *J. Opt. Soc. Am.*, 1971, **61**, 1101–1111.
- 3 J. P. Desclaux and B. Fricke, *J. Phys.*, 1980, **41**, 943–946.
- 4 Y. Zou and C. Froese Fischer, *Phys. Rev. Lett.*, 2002, **88**, 183001.
- 5 A. Kramida, Yu. Ralchenko, J. Reader and the NIST ASD Team, *Atomic Spectra Database (ver. 5.2)*, 2016, v 5.2.
- 6 X.-Y. Cao and M. Dolg, *Mol. Phys.*, 2003, **101**, 961–969.
- 7 W. Brüchle, M. Schädel, U. W. Scherer, J. V. Kratz, K. E. Gregorich, D. Lee, M. Nurmi, R. M. Chasteler, H. L. Hall, R. A. Henderson and D. C. Hoffman, *Inorg. Chim. Acta*, 1988, **146**, 267–276.
- 8 D. C. Hoffman, R. A. Henderson, K. E. Gregorich, D. A. Bennett, R. M. Chasteler, C. M. Chasteler, C. M. Gannett, H. L. Hall, D. M. Lee, M. Nurmi, S. Cai, R. Agarwal, A. W. Charlop, Y. Y. Chu, G. T. Seaborg and R. J. Silva, *J. Radioanal. Nucl. Chem.*, 1988, **124**, 135–144.



9 U. W. Scherer, J. V. Kratz, M. Schädel, W. Brückle, K. E. Grigorich, R. A. Henderson, D. Lee, M. Nurmia and D. C. Hoffman, *Inorg. Chim. Acta*, 1988, **146**, 249–254.

10 M. R. MacDonald, J. E. Bates, J. W. Ziller, F. Furche and W. J. Evans, *J. Am. Chem. Soc.*, 2013, **135**, 9857–9868.

11 E. Eliav, U. Kaldor and Y. Ishikawa, *Phys. Rev. A: At., Mol., Opt. Phys.*, 1995, **52**, 291–296.

12 R. Ahuja, A. Blomqvist, P. Larsson, P. Pyykkö and P. Zaleski-Ejgierd, *Phys. Rev. Lett.*, 2011, **106**, 018301.

13 S. Fritzsche, C. Z. Dong, F. Koike and A. Uvarov, *Eur. Phys. J. D*, 2007, **45**, 107–113.

14 L. Pauling, *The Nature of the Chemical Bond*, Cornell Univ. Press, Ithaca, NY, 3rd edn, 1960.

15 J. P. Desclaux, *At. Data Nucl. Data Tables*, 1973, **12**, 311–406.

16 B. Vest, K. Klinkhammer, C. Thierfelder, M. Lein and P. Schwerdtfeger, *Inorg. Chem.*, 2009, **48**, 7953–7961.

17 K. Balasubramanian, *J. Chem. Phys.*, 2002, **116**, 3568–3575.

18 S. Dubillard, J.-B. Rota, T. Saue and K. Faegri, *J. Chem. Phys.*, 2006, **124**, 154307.

19 W.-H. Xu, X. Jin, M.-H. Chen, P. Pyykkö, M.-F. Zhou and J. Li, *Chem. Sci.*, 2012, **3**, 1548–1554.

20 W. B. Jensen, *Found. Chem.*, 2015, **17**, 23–31.

21 L. Lavelle, *J. Chem. Educ.*, 2008, **85**, 1482–1483.

22 P. Pyykkö, *J. Phys. Chem. A*, 2015, **119**, 2326–2337.

23 IUPAC, iupac.org/what-we-do/periodic-table-of-elements/, Downloaded 4 May 2016.

24 E. van Lenthe, E. J. Baerends and J. G. Snijders, *J. Chem. Phys.*, 1993, **99**, 4597–4610.

25 J. P. Perdew, K. Burke and M. Ernzerhof, *Phys. Rev. Lett.*, 1996, **77**, 3865–3868.

26 E. van Lenthe and E. J. Baerends, *J. Comput. Chem.*, 2003, **24**, 1142–1156.

27 J. Tao, J. P. Perdew, V. N. Staroverov and G. E. Scuseria, *Phys. Rev. Lett.*, 2003, **91**, 146401.

28 V. Staroverov, G. Scuseria, J. Tao and J. Perdew, *J. Chem. Phys.*, 2003, **119**, 12129–12137.

29 A. Klamt and G. Schüürmann, *J. Chem. Soc., Perkin Trans. 2*, 1993, 799–805.

30 ADF2016, SCM, Theoretical Chemistry, Vrije Universiteit, Amsterdam, The Netherlands, <http://www.scm.com>.

31 G. te Velde, F. M. Bickelhaupt, E. J. Baerends, C. Fonseca Guerra, S. J. A. van Gisbergen, J. G. Snijders and T. Ziegler, *J. Comput. Chem.*, 2001, **22**, 931–967.

32 TURBOMOLE V7.02 2015, a development of University of Karlsruhe and Forschungszentrum Karlsruhe GmbH, 1989–2007, TURBOMOLE GmbH, since 2007; available from <http://www.turbomole.com>.

33 S. Knecht and T. Saue, X2Cmod: A modular code for Exact-Two-Component Hamiltonian Transformations. 2010–2013 with contributions from M. Ilias, H. J. Aa. Jensen and M. Repisky, 2010.

34 J. K. Laerdahl, T. Saue and K. Faegri Jr, *Theor. Chem. Acc.*, 1997, **97**, 177–184.

35 L. Visscher, T. J. Lee and K. G. Dyall, *J. Chem. Phys.*, 1996, **105**, 8769–8776.

36 R. Bast, T. Saue, L. Visscher, H. J. A. Jensen *et al.*, DIRAC, a relativistic *ab initio* electronic structure program, Release DIRAC15 (2015), see <http://www.diracprogram.org>.

37 H.-J. Werner, P. Knowles, G. Knizia, F. Manby and M. Schütz, *et al.* MOLPRO, version 2015.1, a package of *ab initio* programs, 2015, see <http://www.molpro.net>.

38 H.-J. Werner, P. J. Knowles, G. Knizia, F. R. Manby and M. Schütz, *Wiley Interdiscip. Rev.: Comput. Mol. Sci.*, 2012, **2**, 242–253.

39 K. G. Dyall, *Theor. Chem. Acc.*, 2012, **131**, 1–11.

40 X.-Y. Cao and M. Dolg, *J. Chem. Phys.*, 2001, **115**, 7348–7355.

41 X.-Y. Cao, M. Dolg and H. Stoll, *J. Chem. Phys.*, 2003, **118**, 487–496.

